Phase control of photon-echo dynamics with overlapping pulse pairs

Sharad Joshi,[1] Carl R. Pidgeon,[1] Ben N. Murdin,[2] and Ian Galbraith[1]

[1]*Institute of Photonics and Quantum Sciences, SUPA, School of Engineering and Physical Sciences, Heriot-Watt University, Edinburgh EH14 4AS, United Kingdom*

[2]*Advanced Technology Institute and SEPNet, University of Surrey, Guildford, Surrey GU2 7XH, United Kingdom*

(Received 5 August 2016; published 30 January 2017)

We report on the dynamics of two-pulse photon echoes in a two-level system. We consider two different types of excitation pulse pairs: pulses with the same carrier envelope phases (CEP pulse pairs) and pulse pairs cut from the same carrier wave train (labeled as normal pulse pairs). We show that for CEP pulse pairs when the pulses overlap somewhat the photon-echo emission time is strongly sensitive to the relative phase (i.e., delay time) between the two pulses. We also show how the photon-echo emission time for such CEP pulse pairs depends on the dephasing time of the polarization (T_2) and the pulse width of the applied pulses. This phase sensitivity can be utilized to control the emission time of the photon echo which may prove useful in storing and retrieving light signals from an atomic ensemble. Our results also inform the interpretation of photon-echo signals at short delay time when used to measure fast coherence decay rates.

DOI: 10.1103/PhysRevA.95.013416

I. INTRODUCTION

Spin echoes, also known as Hahn echoes [1], were first detected by Erwin Hahn in 1950. These echoes originate from the rephasing of spin coherence after the application of a pair of radio frequency excitation pulses delayed by time τ_d. A photon echo is similarly the rephasing of the optical polarization after optical excitation by a pulse pair. Echoes have important applications in many fields including spectroscopy [2,3], quantum information processing [4], studying magnons and phonons in single crystals [5], and measurement of spin-spin or polarization relaxation times (T_2) [6]. The photon echo is one potential candidate for quantum storage of light in an atomic ensemble and photon echoes are being investigated for application in long-term optical quantum memories [7–9]. Conventional photon echoes have low signal retrieval efficiency [10] and the time of the echo appearance after the second pulse is fixed near to the interpulse delay. Techniques for on-demand retrieval of the photon echo would be beneficial [11,12] and techniques like controlled reversible inhomogeneous broadening (transverse as well as longitudinal) are being developed to increase the signal retrieval efficiency of such systems [13]. Even after 65 years, the interest in echo phenomena is still rising as further applications emerge; therefore it is imperative that we study and understand all aspects of photon-echo dynamics.

In this paper, we study the echo dynamics for two different kinds of pulse pairs. For pulse pairs that each have the same carrier envelope phase, denoted *CEP* pulse pairs, the electric field can be written as

$$E(t) = \sum_{j=1,2} E_j(t) = \sum_{j=1,2} \mathcal{E}_j e^{-(t-t_j)^2/2\delta^2} \cos[\omega(t-t_j)],$$

where $\mathcal{E}_j$ is the pulse peak amplitude, t_j locates the pulse Gaussian envelope in time, ω is the driving laser frequency, and δ is the temporal pulse width. Typically $\mathcal{E}_1$,$\mathcal{E}_2$ and δ are chosen to yield $\pi/2$ and π pulse areas respectively but this is not crucial to the photon echo phenomenon. For pulse pairs that are cut out from the same carrier wave train, denoted here as *normal* pulses, the electric field can be written as

$$E(t) = \sum_{j=1,2} \mathcal{E}_j e^{-(t-t_j)^2/2\delta^2} \cos[\omega(t-t_1)].$$

Figure 1 illustrates these two different kinds of pulse pairs. We see that the phasing of the envelope and the carrier wave of both pulses in a CEP pulse pair is identical, whereas for normal pulse pairs this is not the case. Most of the studies (and applications hitherto) of photon and spin echoes consider only nonoverlapping pulses. By exploring the regime where pulses partially overlap, we found that the photon-echo signal is very sensitive to the *relative* phase (i.e., interpulse delay, τ_d) between the pulses when a CEP pulse pair is used. Unsurprisingly the absolute value of the carrier envelope phase has no influence on the echo dynamics other than defining the phase of the underlying polarization oscillations. Using numerical simulations and approximate analytic solutions to the optical Bloch equations we find that large shifts in the echo emission time are possible by controlling parameters such as the delay between the pulses, the inhomogeneous broadening of the two-level ensemble, the pulse widths of the applied pulses, and the polarization dephasing time.

Results from this study show that we can achieve control over the emission time of the echo signal while using the same pulse sequence ($\pi/2$-π) as the conventional echoes. This wasn't possible before in a two-level system. Therefore, just by overlapping the pulses we can increase the storage time of the signal (limited by T_2) by a significant amount as shown in the numerical simulations in Sec. III.

Photon-echo experiments which attempt to measure dephasing times which are close to the available pulse durations will naturally make some measurements with partially overlapping excitation pulses. Our results show that, depending on the relative phase difference between the pulses, strongly shifting (in time) photon echoes will arise. This may be misinterpreted as jitter or noise when, as we show, it is in fact a consequence of interference.

We next distinguish our results from previous published results where the phase difference between pairs of

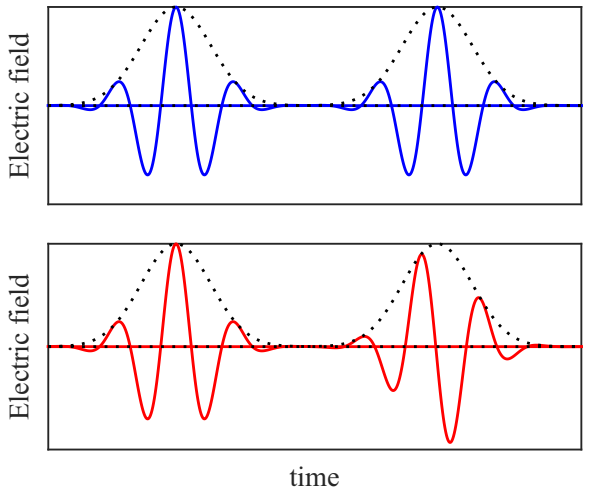

FIG. 1. Illustration of a CEP pulse pair (top panel) and a normal pulse pair (bottom panel). The Gaussian envelope (dotted line) highlights the difference between CEP and normal pulses.

excitation pulses have proven useful in nonlinear spectroscopy. Reference [2] shows how the real and imaginary parts of the nonlinear response function can be measured independently using nonoverlapping phase-locked pulses by changing the phase between the two pulses to be in-phase and in-quadrature. Using heterodyne-detected phase-locked femtosecond stimulated photon-echo and phase-locked, pump-probe techniques [14,15] it has been shown that the relative phase between two initial pulses and the relative phase between the last two pulses are both important individually rather than only their difference. Here again the second and third pulses never overlap in time. A shift in echo maximum with delay between the pulses is plotted and a quantum beatlike pattern is shown on the scale of 1 ps with a pulse width of 14 fs, i.e., much longer than the frequency and therefore not an interference phenomenon. A deformation of pulses when overlapped in the time domain is not considered here, which is the distinguishing feature in the present paper. The paper of Yano and Shinojima [16] considers a comparison between CEP and normal pulses for photon echoes and coherent population control using a perturbative approach which neglects any pulse overlap. Their results predict a shift in echo temporal position with respect to pulse widths when the dephasing and decay times differ, but this shift does not arise from the changing overlap between the pulses (as this is neglected from the start).

In coherent photon-echo simulations, there are five independent energy and time quantities which come into play: (i) the interpulse delay, (ii) the pulse widths, (iii) the inhomogeneous linewidth, (iv) the detuning of the excitation from the center of the inhomogeneous line, and (v) the dephasing time. In this large phase space there is no natural scaling, so we choose to present simulations for physical parameters corresponding to the $1s$-$2p_+$ transitions of phosphorus-doped silicon (Si:P) which has potential for quantum information processing [17,18]. The behavior we report however is generic and can be easily applied with appropriate scaling to other materials and systems.

II. PHOTON-ECHO BLOCH EQUATIONS

The Bloch equations for a single two-level system in the rotating frame of the driving field $E(t)$ can be written [19] as

$$\frac{dn_g}{dt} = i\sum_j \frac{\Omega_j(t)}{2}[P_{ge}e^{i\phi_j} - P_{ge}^* e^{-i\phi_j}] + \frac{n_e}{T_1}, \quad (1)$$

$$\frac{dn_e}{dt} = -i\sum_j \frac{\Omega_j(t)}{2}[P_{ge}e^{i\phi_j} - P_{ge}^* e^{-i\phi_j}] - \frac{n_e}{T_1}, \quad (2)$$

$$\frac{dP_{ge}}{dt} = i\sum_j \frac{\Omega_j(t)}{2} e^{-i\phi_j}(n_g - n_e) + iP_{ge}(\omega_0 - \omega) - \frac{P_{ge}}{T_2}, \quad (3)$$

where the summation over j covers multiple pulses, n_g is the population of the ground state, n_e is the population of the excited state, ω_0 is the transition frequency, P_{ge} is the polarization, $\Omega_j(t) = dE_j(t)/\hbar$ quantifies the effect of the driving pulses on the transition dipole d, ϕ is the phase difference between the two pulses of the pair, and T_1 and T_2 are, respectively, the population and polarization radiative relaxation times with $T_1 = 2T_2$. In the case of normal pulses, $\phi = 0$, and for CEP pulses $\phi = \omega\tau_d$, where τ_d is the delay between the pulses.

To include the influence of different local environments (i.e., inhomogeneous broadening) we simply solve the Bloch equations for two-level systems having a distribution of transition frequencies. Integrating over this distribution yields the total polarization, P_{total}, for an ensemble of systems with the chosen inhomogeneous broadening, i.e.,

$$P_{\text{total}} = \int^{\Delta'} P_{ge}(\Delta')\, g(\Delta')\, d\Delta', \quad (4)$$

where Δ' is the detuning between transition and driving frequencies and $g(\Delta')$ is the normalized inhomogeneous distribution of two-level atoms with

$$g(\Delta') = \mathcal{G}\, e^{-(\Delta'-\Delta)^2/(2\sigma^2)}. \quad (5)$$

In all our simulations the center frequency of the pulses is chosen to coincide with the center of the inhomogeneous distribution.

III. NUMERICAL SIMULATIONS

Here we present numerical simulations of Eqs. (1)–(5) to investigate the dependence of the photon-echo emission dynamics on parameters such as the relative phase between the pulse pair, pulse duration, and dephasing. All the simulations in this paper are for CEP pulses unless otherwise noted.

A. Photon-echo dynamics for partially overlapping pulses

In Fig. 2 we show the absolute value of the polarization for a case where the two pulses partially overlap in time for different pulse interference conditions, i.e., when pulses interfere constructively or destructively. We see a large shift ($\approx$13 ps) in the arrival time of the echo even when the delay between the pulses is changed by only 0.05 ps, a very small fraction of the interpulse delay of around 33.4 ps.

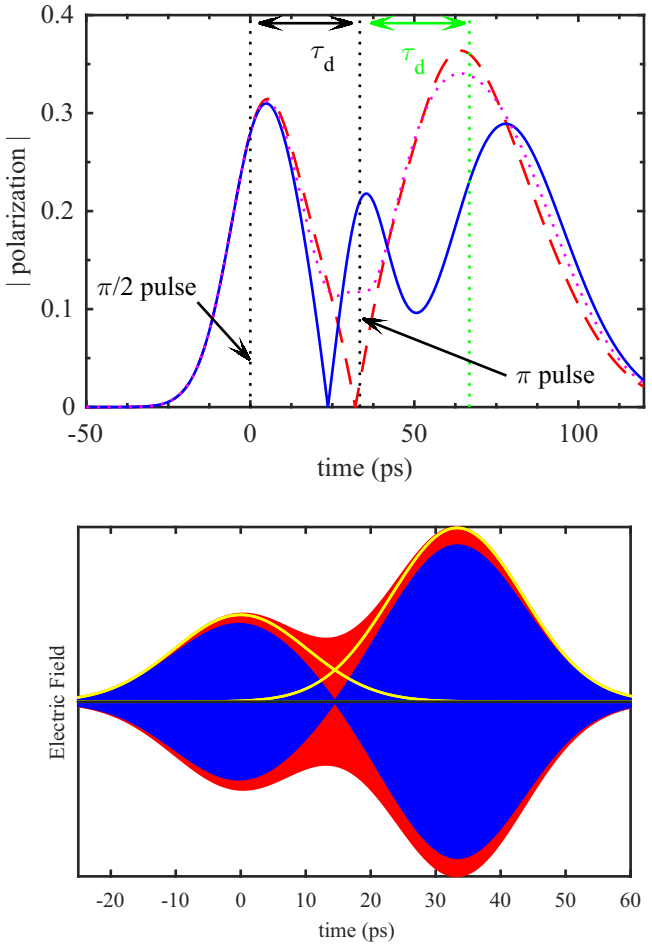

FIG. 2. (Upper panel) Absolute value of the polarization vs time for different delays (τ_d) between the CEP pulses. The solid blue line is the destructive interference, $\tau_d = 33.4057$ ps. The dashed red line is the constructive interference, $\tau_d = 33.3531$ ps. The dotted magenta line is the quarter of an oscillation, $\tau_d = 33.3794$ ps. The transition frequency is 9.504 37 THz, the detuning is zero, and the first pulse has an area of $\pi/2$ and the second an area of π. The intensity full width at half maximum (FWHM) pulse width of both pulse envelopes is 17 ps, the FWHM inhomogeneous broadening is 0.028 THz, and the dephasing time T_2 is infinite. $t = 0$ corresponds to the arrival of the peak of the first pulse. (Lower panel) Illustration of net driving electric field from overlapping $\pi/2$ and π pulses under constructive red (light) and destructive blue (dark) interference conditions. Individual pulse envelopes are shown as the solid yellow lines and the fast carrier frequency oscillation is not resolved. The amplitude of the destructive interference case has been reduced by 10% for clarity.

To get the full picture of how the echo signal is changing with respect to the delay between the pulses we solved the Bloch equations numerically for many different delays and plotted the echo signal as a heat map as shown in Fig. 3. This shows that the echo peak position and to a lesser extent the echo strength are very sensitive to the relative phase between the pulses.

When pulses do not overlap in the time domain we do not observe this phase sensitivity of the echo signal emission time whether the pulses used are CEP or normal. So the observed delay sensitivity is only seen for partially overlapping CEP

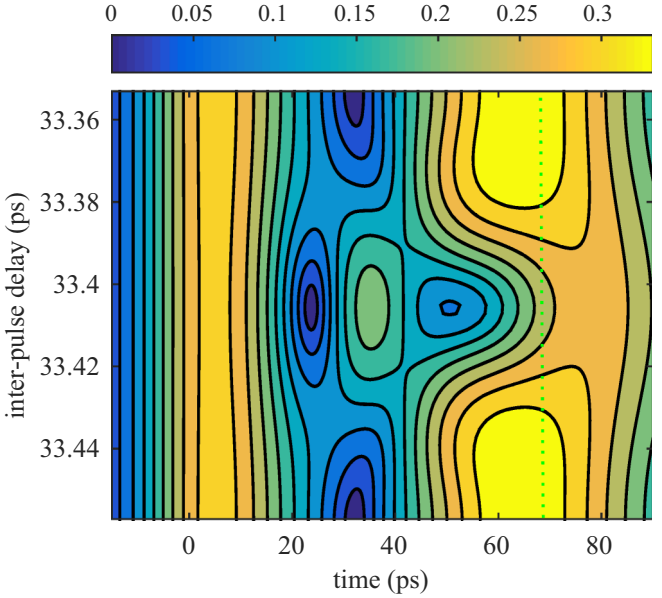

FIG. 3. Heat map of absolute value of polarization versus time for different delays (τ_d) between the pulses for photon echo using CEP pulses. The green dotted line indicates the time τ_d after the second pulse peak. Parameters are as in Fig. 2.

pulses. This indicates that the origin of the phase sensitivity lies in the interference between the electric fields of the pulses and not between the polarization oscillation induced by the first pulse interfering with the second pulse. The result of such interference is seen in the lower panel of Fig. 2; the constructive interference case (red, light shading) resembles a single pulse with an amplitude modulation while the nodal structure in the destructive interference case (blue, dark shading) produces two slightly shorter but sequential pulses. We use this observation to construct an analytical model of the system in Sec. IV.

This phase sensitivity has implications for the use of photon-echo techniques to measurements of dephasing (T_2) times. If the dephasing times are similar to the pulse length, care must be taken to either use normal pulse pairs or to account for the phase difference between the pulses in the analysis.

B. Influence of pulse overlap area

We next investigate how the area of overlap between the pulses quantitatively affects the photon-echo emission time and its dependence on the relative phase between the two pulses. This overlap area can be changed by either (i) changing the pulse width keeping the delay between the applied pulses constant or (ii) changing the delay between the applied pulses while keeping the pulse width constant.

Figure 4 shows the effect of changing the pulse width while keeping all other parameters, including the pulse areas, fixed. For destructive interference, around $\tau_d = 33.4$ ps, as we increase the pulse width the shift in the echo peak position in time increases by over 15 ps. Also interesting are the qualitative changes that increasing the pulse width brings midway between constructive and destructive interference conditions around a delay of $\tau_d = 33.43$ ps; the echo peak position is not even monotonic with the pulse width. For

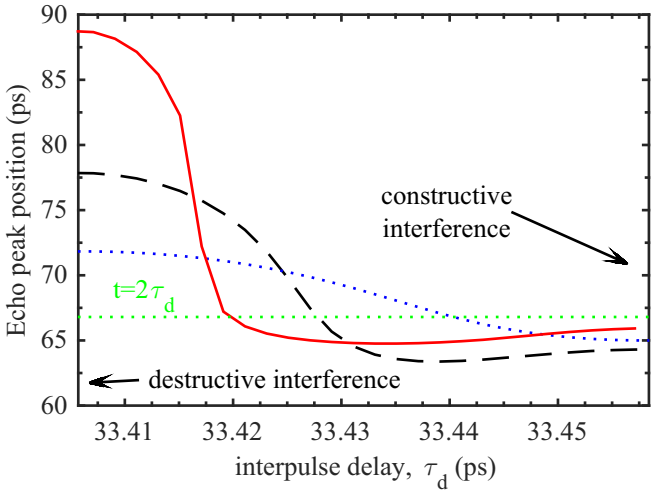

FIG. 4. Echo peak position in time vs delay between the pulses for different (intensity) pulse durations: dotted blue line, FWHM = 12 ps; dashed black line, FWHM = 17 ps; and red line, FWHM = 23.5 ps. Across the figure the interference condition passes from destructive (left) to constructive (right). The horizontal green dotted line indicates the time τ_d after the second pulse peak. Other parameters are as in Fig. 2.

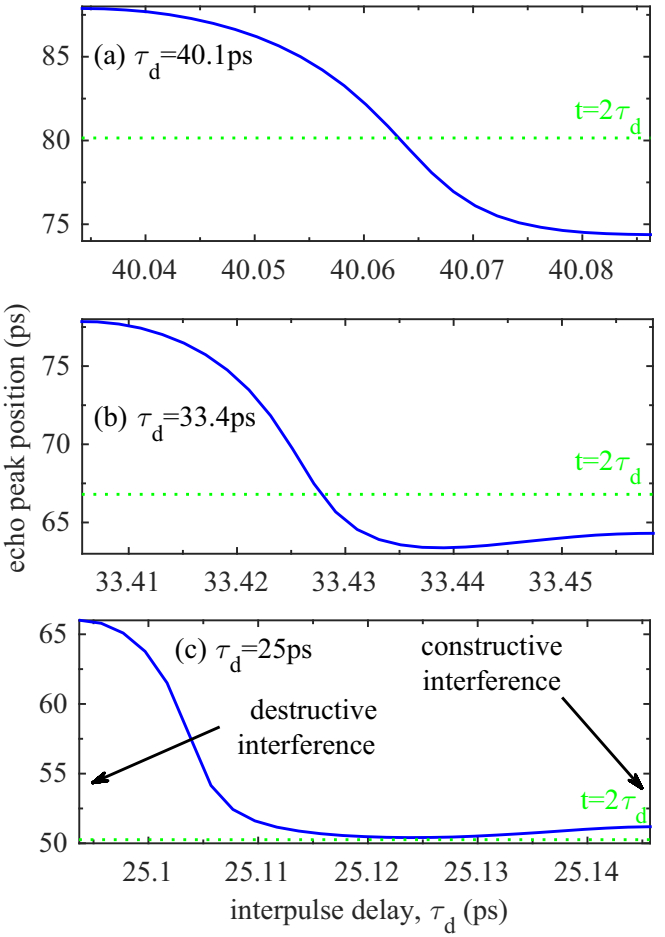

FIG. 5. Echo peak position in time vs delay between the pulses for different delays around (a) $\tau_d = 40.1$ ps, (b) $\tau_d = 33.4$ ps, and (c) $\tau_d = 25$ ps. Across the figure the interference condition passes from destructive (left) to constructive (right). The green dotted line indicates the time τ_d after the second pulse peak. Other parameters are as in Fig. 2.

constructive interference the shifts seen are rather small, indicating an insensitivity to pulse width in this regime.

Figure 5 shows the photon-echo peak position in time versus delay between the pulses for a fixed (intensity) pulse duration of 17 ps (FHWM). We show scans from destructive interference through to constructive interference for three different delays around (a) $\tau_d = 40$ ps, (b) $\tau_d = 33.4$ ps, and (c) $\tau_d = 25.1$ ps. The change in overlap area of the two pulses is negligible within one scan but appreciable between the three subplots. We can see that here also the qualitative nature of the echo signal changes as we increase the delay; for shorter delays constructive interference echoes are emitted at times later than those for mixed quadrature excitation. Overall, for all interference conditions, longer pulse excitation tends to bring the emission back towards the $t = 2\tau_d$ line.

We conclude from these simulations that it is the specific combination of pulse width and interpulse delay that determines the qualitative behavior of echo, not simply the area of overlap between the pulses. We have also run simulations where by changing both the pulse duration and the interpulse delay we hold the pulse overlap constant and find no universal dependence on the overlap area.

IV. ANALYTICAL FORMULAS FOR PHOTON-ECHO SIGNALS

In this section we describe three special cases where we can derive an analytical formula for the shifts in the position of photon echo in the CEP case. The electric field of the pulses are assumed to be top hat in time and have the same amplitude. The second pulse is twice as long as the first and thus has the required area for a π pulse. The three cases are (i) when the applied pulses do not overlap, (ii) when the applied pulses interfere destructively, and (iii) when the applied pulses interfere constructively.

A. Nonoverlapping pulses

For comparison in the case where pulses do not overlap in time there is an existing result [19],

$$P(t_4) = -2\mathcal{P}_0\, e^{-\sigma^2(t_{43}-t_{21}-1/\Omega_1)^2/2}\, \sin(\omega t_4), \qquad (6)$$

where $P(t_4)$ is the polarization after the application of the second pulse, $\mathcal{P}_0$ is a constant, and Ω_1 is the Rabi frequency of the initial $\pi/2$ pulse. t_{21} is the time interval between the two pulses and t_{43} is the time coordinate relative to the end of the second pulse. The echo appears when these two are almost equal, with a small correction due to the finite pulse width.

B. CEP pulses: Destructive interference

In this case the total electric field can be written as a piecewise constant field of varying amplitude [see Fig. 6(a)]. When the pulses overlap the electric field is zero so instead

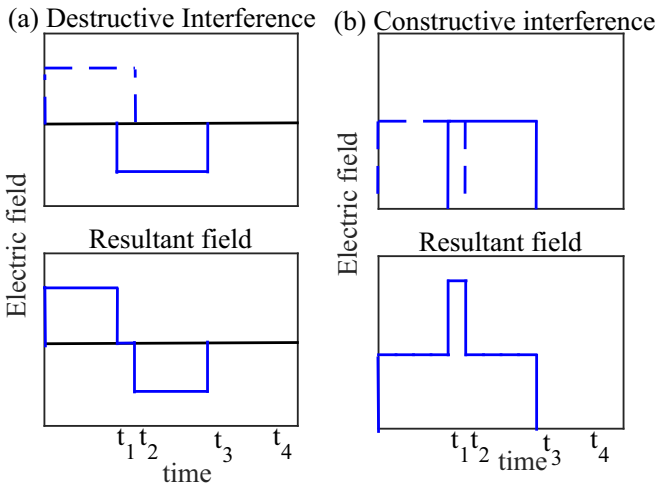

FIG. 6. The envelope of two top hat pulses interfering (a) destructively and (b) constructively. The destructive interference provides a region of zero field when the pulses are overlapping which allows an interval of free polarization oscillation and rephasing. For the constructive case, interference in the interval (t_1, t_2) causes the amplitude of the electric field to double at those times. In effect this results in three consecutive finite field regions.

of overlapping $\pi/2$ and π pulses we have two pulses with smaller area and a period of free nutation in between. This gives rise to a modified echo which is the origin of the phase control of the photon-echo dynamics we report here. In each section of the pulse sequence, we can write the solution in the Rabi form and by multiplying the matrices together an analytic solution for the polarization can be found. This only works for perfectly constructive or destructive interference but still we can gain some insight by studying these limits. Following the same calculation as in Ref. [19] but with CEP pulses, we derive the result for destructively interfering pulses:

$$P(t_4) = \mathcal{P}_0[\cos A(e^{-\sigma^2(t_{43}+t_{21}-C)^2/2} - e^{-\sigma^2(t_{43}-t_{21}-C)^2/2}) - \cos^2 A(e^{-\sigma^2(t_{43}+t_{21}+D)^2/2} + e^{-\sigma^2(t_{43}-t_{21}+D)^2/2}) + 2\sin^2 A e^{-\sigma^2(t_{43}+E)^2/2}] \sin(\omega t_4), \quad (7)$$

with

$$C = (1+\sin 2A)/\Omega_1,$$
$$D = (\sin A \sec^2 A - \sec^2 A - \tan A)/\Omega_1,$$
$$E = (\cot A + \csc A)/\Omega_1,$$

where A is the area of overlap between the pulses (between 0 and $\pi/2$), ω is the applied laser frequency, and $t_{21} = t_2 - t_1$ and $t_{43} = t_4 - t_3$ are the times as shown in Fig. 6. As area A is always less than $\pi/2$, C and E are always positive, while D is always negative. Superposition of the first four terms in the formula defines the echo profile and the arrival time, while the last term doesn't actually contribute to the echo signal after time t_3 because E is always positive, which implies that the peak of the Gaussian lies before t_3 and hence does not affect the echo that comes at times later than t_3. The shift in the position of echo depends on the area of overlap (A) between the pulses and the Rabi frequency of the applied pulses. For $A = 0$ this result reduces to Eq. (6) as it must.

Equation (7) describes well the observed behaviors for destructive interference. Increasing the pulse duration for a fixed delay, or decreasing the delay time for a fixed pulse duration, increases the pulse overlap area A. As A increases, C becomes larger and D more negative and both these trends lead to an increase in the shift of the echo emission time. Both these trends are seen in the full numerical simulations of Figs. 4 and 5.

The FWHM of each term is inversely related to the FWHM of the inhomogeneous broadening distribution, i.e., the broader the ensemble linewidth (larger σ), the narrower the Gaussians in each term of the formula. Therefore, the superposition between these four terms will change if we change the inhomogeneous broadening distribution. This implies that the echo position also depends on the ensemble linewidth. Now by controlling the area of overlap between the pulses as well as the pulse width, we can have control over the emission time of the echo, which might be important in storing light using atomic ensembles.

C. CEP pulses: Constructive interference

For constructive interference between the CEP pulses [see Fig. 6(b)], we find

$$P(t_4) = -\mathcal{P}_0\, e^{-\sigma^2(t_{43}-1/\Omega_1)^2/2} \sin(\omega t_4).$$

This result is independent of the overlap between the pulses, which is consistent with the rather weak shifts seen for constructive interference in Figs. 4 and 5. This formula is only valid when $A \neq 0$ and therefore it is not equivalent to Eq. (6). Effectively within this analytic model there is no real echo emitted. This can be understood by noting that there is no free precession interval (the electric field in the interval t_{21} is not zero) between the two pulses. This means the macroscopic polarization does not have time to freely unphase; therefore we do not get a distinct photon-echo signal from the rephasing of oscillators after the excitation pulses are gone.

V. THE INFLUENCE OF DEPHASING

In Fig. 7 we show the effect of introducing a finite polarization dephasing time, $T_2 = 120$ ps, on the echo peak position in time. For destructive interference we find that the finite dephasing time shifts the curve to earlier times while for constructive interference we find essentially no effect. For shorter pulses (not shown) there is also a shift for constructive interference to earlier times too, but a full exploration of this phase space is beyond the scope of this paper.

Photon-echo decay with a nonoverlapping $(\frac{\pi}{2},\pi)$ pulse sequence is the conventional technique to measure the polarization relaxation times (T_2). The echo signal strength is measured for a range of interpulse delays, and an exponential decay in strength (with the rate of decay depending on T_2) is observed. Such measurements are most easily done when the dephasing time is considerably longer than the pulse duration, allowing for time discrimination over a decade or more in signal decay. Our results on the strong phase sensitivity of the echo arrival time inform such measurements in two ways.

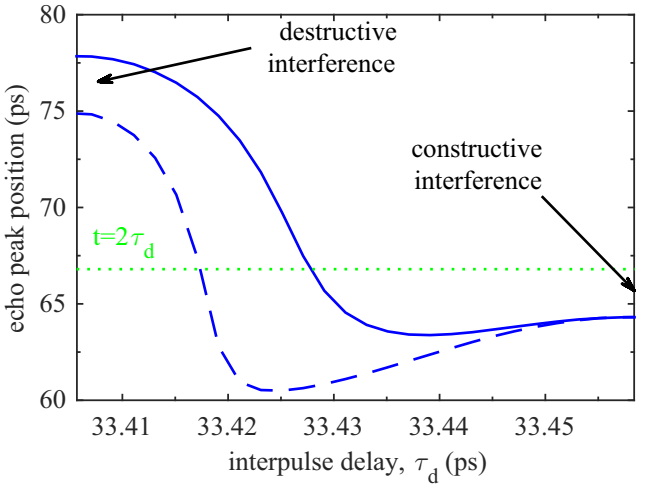

FIG. 7. Echo peak position in time vs delay between the pulses for different dephasing times. The solid line is the infinite dephasing time, and the dashed line is the dephasing time $T_2 = 120$ ps. The green dotted line indicates the time τ_d after the second pulse peak. Other parameters are as in Fig. 2.

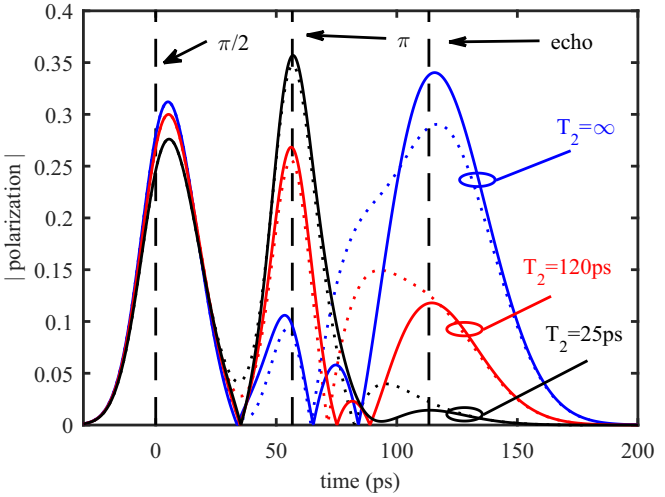

FIG. 8. Polarization amplitude vs time for constructive interference (dotted) and destructive interference (solid lines) delays with $T_2 = \infty$ (blue), $T_2 = 120$ ps (red), and $T_2 = 25$ ps (black). The interpulse delay is 56 ps, the (intensity) FWHM pulse duration is 17 ps, and other parameters are as in Fig. 2.

First at early times when the pulses overlap to some degree, unless care is taken over the precise interpulse phase at each delay selected, there will appear in the data some scatter reflecting the spread of excitation phases used. Without an appreciation of the source of this scatter it may be wrongly interpreted as due to some other source of noise. Second, often it is desirable to push the techniques to measure dephasing times which approach the pulse duration and hence the phase sensitivity reported here would come into play. To explore if new information could be gained with knowledge of the interference condition, we show in Fig. 8 the echo signal for constructive and destructive interference using a range of T_2 values. The FWHM pulse duration is 17 ps, which corresponds to around 24 ps in the field, so with an interpulse delay of 56 ps there is still appreciable overlap between the CEP pulses. The echo signal for destructive interference is distinct and remains identifiable (but reduced in intensity) even for dephasing times similar to the field pulse duration. At constructive interference and for the longest dephasing times the echo peak positions are close to the expected location, whereas for shorter dephasing times the echo signal is mixed in a complex way with the driven polarization of the system. Unraveling what is echo signal and what is driven polarization is impossible, preventing a T_2 determination. This suggests that to measure a fast dephasing time one should measure it using CEP pulses at delays corresponding to destructive interference. In essence one receives an advantage by using the destructive interference to shape the overlapping pulses into two shorter bursts of the electric field.

VI. CONCLUSIONS

To conclude, we have shown numerically and analytically that when carrier-envelope-phase pulses overlap we see a strong phase dependence of the echo position (in time). Shifts of over 10 ps have been seen. The qualitative nature of this phase (delay) dependence changes depending on the pulse overlap area, the pulse width of the applied pulses, the dephasing time, and the inhomogeneous linewidth of the system. In the case of well-separated carrier-envelope-phase pulses, the echo peak position (in time) is independent of the phase difference between the applied pulses. For all normal pulses, the echo peak position (in time) is insensitive to wavelength-scale changes of the delay between the applied pulses. In all cases, there is an inherent small shift in the echo peak position in time due to the finite pulse width of the applied pulses. Our results inform both the interpretation and design of ultrafast polarization relaxation measurements using photon-echo techniques as they guide the interpretation of the measured signals when the pulses overlap. Making photon-echo measurements in the destructive interference condition should allow the resolution of dephasing times shorter than those in the constructive interference configuration.

ACKNOWLEDGMENTS

B.N.M. gratefully acknowledges support from the EPSRC (Grant No. EP/H026622/1, "COMPASS") and a Royal Society Wolfson Merit Award. S.J. acknowledges support from the Scottish Centre for Doctoral Training in Condensed Matter Physics (Grant No. EPL/015110/1).

[1] E. L. Hahn, Phys. Rev. **80**, 580 (1950).
[2] M. Cho, N. Scherer, G. Fleming, and S. Mukamel, J. Chem. Phys. **96**, 5618 (1992).
[3] R. M. Macfarlane, R. M. Shelby, and R. L. Shoemaker, Phys. Rev. Lett. **43**, 1726 (1979).
[4] S. A. Moiseev and W. Tittel, Phys. Rev. A **82**, 012309 (2010).

[5] F. Mezei, Z. Phys. **255**, 146 (1972).
[6] S. Meiboom and D. Gill, Rev. Sci. Instrum. **29**, 688 (1958).
[7] N. Sangouard, C. Simon, M. Afzelius, and N. Gisin, Phys. Rev. A **75**, 032327 (2007).
[8] S. A. Moiseev, Phys. Rev. A **83**, 012307 (2011).
[9] A. I. Lvovsky, B. C. Sanders, and W. Tittel, Nat. Photonics **3**, 706 (2009).
[10] J. Ruggiero, J.-L. Le Gouët, C. Simon, and T. Chanelière, Phys. Rev. A **79**, 053851 (2009).
[11] B. S. Ham, Opt. Express **18**, 1704 (2010).
[12] B. S. Ham, Nature Photonics **3**, 518 (2009).
[13] M. P. Hedges, J. J. Longdell, Y. Li, and M. J. Sellars, Nature (London) **465**, 1052 (2010).
[14] W. de Boeij, M. Pshenichnikov, and D. Wiersma, Chem. Phys. Lett. **238**, 1 (1995).
[15] W. de Boeij, M. Pshenichnikov, and D. Wiersma, Chem. Phys. Lett. **247**, 264 (1995).
[16] R. Yano and H. Shinojima, Phys. B (Amsterdam, Neth.) **407**, 246 (2012).
[17] B. N. Murdin, J. Li, M. L. Y. Pang, E. T. Bowyer, K. L. Litvinenko, S. K. Clowes, H. Engelkamp, C. R. Pidgeon, I. Galbraith, N. Abrosimov *et al.*, Nat. Commun. **4**, 1469 (2013).
[18] K. Litvinenko, E. Bowyer, P. Greenland, N. Stavrias, J. Li, R. Gwilliam, B. Villis, G. Matmon, M. Pang, B. Redlich *et al.*, Nat. Commun. **6**, 6549 (2015).
[19] L. Allen and J. H. Eberly, *Optical Resonance and Two-Level Atoms* (Dover, New York, 1975).